ORIGINAL ARTICLE

Cancer Science WILEY

FAM111B enhances proliferation of *KRAS*-driven lung adenocarcinoma by degrading p16

Keisuke Kawasaki[1] iD | Satoshi Nojima[1] | Sachiko Hijiki[1] | Shinichiro Tahara[1] iD |
Kenji Ohshima[1] | Takahiro Matsui[1] | Yumiko Hori[1] | Masako Kurashige[1] |
Daisuke Umeda[1] | Hiroki Kiyokawa[1] | Kansuke Kido[1] | Daisuke Okuzaki[2,3,4] |
Eiichi Morii[1]

[1]Department of Pathology, Graduate School of Medicine, Osaka University, Osaka, Japan

[2]Single Cell Genomics, Human Immunology, WPI Immunology Frontier Research Center, Osaka University, Osaka, Japan

[3]Research Institute for Microbial Diseases, Genome Information Research Center, Osaka University, Osaka, Japan

[4]Institute for Open and Transdisciplinary Research Initiatives, Osaka University, Osaka, Japan

Correspondence
Eiichi Morii, Department of Pathology, Osaka University Graduate School of Medicine, 2-2 Yamadaoka, Suita, Osaka 565-0871, Japan.
Email: morii@molpath.med.osaka-u.ac.jp

Funding information
Japan Society for the Promotion of Science, Grant/Award Number: A19H034520, T17K195550, T18K150780, T18K150790, T19K165570 and T19K165850

Abstract

Lung cancer is a common type of cancer that represents a health problem worldwide; lung adenocarcinoma (LUAD) is a major subtype of lung cancer. Although several treatments for LUAD have been developed, the mortality rate remains high because of uncontrollable progression. Further biological and clinicopathological studies are therefore needed. Here, we investigated the role of family with sequence similarity 111 member B (FAM111B), which is highly expressed in papillary-predominant LUAD; however, its role in cancer is unclear. An immunohistochemical analysis confirmed that papillary-predominant adenocarcinomas exhibited higher expression of FAM111B, compared with lepidic-predominant adenocarcinomas. Additionally, FAM111B expression was significantly correlated with clinical progression. In vitro functional analyses using FAM111B-knockout cells demonstrated that FAM111B plays an important role in proliferation and cell cycle progression of *KRAS*-driven LUAD under serum-starvation conditions. Furthermore, FAM111B regulated cyclin D1-CDK4-dependent cell cycle progression by degradation of p16. In summary, we revealed the clinical importance of FAM111B in human tumor tissues, as well as its function as a degradative enzyme. Therefore, FAM111B has potential as a clinicopathological prognostic marker for LUAD.

KEYWORDS

cell cycle, FAM111B, lung adenocarcinoma, p16, proliferation

1 | INTRODUCTION

Cancer is a major public health problem worldwide, and lung carcinoma is the leading cause of cancer-related deaths.[1] Adenocarcinoma is the most common histological class of lung carcinoma, and its incidence is increasing.[2] According to the World Health Organization, the 5 subtypes of LUAD are lepidic, acinar, papillary, micropapillary, and solid predominant.[3] Lepidic-predominant adenocarcinomas are composed of (typically bland) non-mucinous adenocarcinoma cells, which grow along the alveolar walls; this subtype has an invasive

---

focus of >0.5 cm, is >3 cm in size, or shows vessel/pleura infiltration.[3] In contrast, papillary-predominant adenocarcinomas are mostly composed of neoplastic cells lining fibrovascular cores of varying size.[3,4] The histological subtypes are associated with prognosis in early stage disease; the lepidic subtype is associated with a good prognosis, the acinar and papillary subtypes are associated with an intermediate prognosis, and the micropapillary and solid subtypes are associated with a dismal prognosis.[3,5-8] Additionally, activating mutations of the *KRAS* proto-oncogene occur in roughly 30% of human LUADs.[9,10] Although such oncogenes and their pathological roles in LUADs have been investigated, the mechanisms of malignant LUAD progression remain unclear.

Homo sapiens family with sequence similarity 111, member B (FAM111B) encodes a protein with a trypsin-like cysteine/serine peptidase domain. FAM111B mutations cause a rare autosomal dominant disease, known as hereditary fibrosing poikiloderma.[11,12] The precise molecular function of FAM111B is unclear, but Sun et al reported that FAM111B is involved in the p53 signaling pathway and might be an oncogene; thus, it may be a useful therapeutic target in patients with LUAD.[13] However, the clinicopathological significance of FAM111B is unknown, especially in terms of the relationship between the histologic classification of LUAD and expression of FAM111B in clinical specimens.

In this study, an immunohistochemical analysis was performed to assess the clinicopathological significance of FAM111B in clinical specimens. Moreover, FAM111B-knockout cells were generated; studies of these cells revealed that FAM111B degrades p16 and regulates the proliferation and cell cycle progression of LUAD cells.

2 | MATERIALS AND METHODS

2.1 | Antibodies

Antibodies were obtained from the following sources: an antibody to FAM111B (HPA038637) was obtained from Atlas Antibodies AB (Bromma, Sweden); antibodies to p15 (ab53034) and CDK4 (ab7955) were purchased from Abcam (Cambridge, MA, USA); antibodies to Rb (#9309), phospho-Rb (Ser807/811; #9308), phospho-mTOR (Ser2448; #2971), mTOR (#2972), phospho-Akt (Ser473; #9271), Akt (#9272), phospho-p44/42 MAPK (Erk1/2, Thr202/Thr204; #4370), p44/42 MAPK (Erk1/2; #9102), p16 (#92803), lamin A/C (#2032), and β-actin (HRP-conjugated; #5125) were obtained from Cell Signaling Technology (Danvers, MA, USA); an antibody to Cyclin D1 (241R) was obtained from Cell Marque (Rocklin, CA, USA); an antibody to E2F-1 (NB600-210) was obtained from Novus Biologicals (Littleton, CO, USA); an antibody to p53 (NCL-L-p53-DO7) was obtained from Leica Biosystems (Wetzlar, Germany); an antibody to FLAG (F3165) was obtained from Sigma-Aldrich (St. Louis, MO, USA); an antibody to Ki-67 (M7240) was obtained from Dako (Glostrup, Denmark); and an antibody to V5 (M215-3) and secondary antibodies (anti-mouse [330] and anti-rabbit [458]) were obtained from Medical & Biological Laboratories (Nagoya, Japan).

2.2 | Plasmids

The plasmids Empty-FLAG (pCMV-3xFLAG), FAM111B-3xFLAG (pCMV-FAM111B-3xFLAG), FAM111BΔTPD-FLAG (pCMV-FAM111BΔTPD-3xFLAG), and p16-V5 (pCMV-p16-V5) were created by Vector Builder, Inc (Chicago, IL, USA).

2.3 | Cell culture

For culture under standard conditions (FCS replete), A549 cells were cultured in DMEM (Nacalai Tesque; Kyoto, Japan) supplemented with 10% FCS (Biowest; Nuaillé, France), penicillin (100 IU/mL), and streptomycin (100 μg/mL). HCC827, H1650, and H1792 cells were cultured in RPMI 1640 medium (Nacalai Tesque) supplemented with 10% FCS, penicillin (100 IU/mL), streptomycin (100 μg/mL), and 2-mercaptoethanol (0.01%). All cells were maintained at 37°C in 5% CO_2.

2.4 | Patients

The study protocol was approved by the Ethics Review Board of Osaka University Hospital (No. 15234) and all experiments were performed in accordance with the institutional guidelines and regulations. Informed consent was obtained from all patients prior to inclusion in the study. We examined 95 patients who underwent surgery for LUAD at Osaka University Hospital from 2013 to 2018. Resected specimens were fixed in 10% formalin and processed for paraffin embedding. Specimens were stored at room temperature in a dark room, sectioned at 4-μm thickness, and subjected to immunohistochemical analysis.

2.5 | Histological evaluation

Hematoxylin and eosin-stained slides of each LUAD were reviewed. Each adenocarcinoma was classified with respect to the dominant pattern (lepidic, papillary, acinar, solid, or invasive mucinous adenocarcinoma).

2.6 | Immunohistochemistry

Formalin-fixed and paraffin-embedded (FFPE) tissues were sectioned and processed; immunohistochemistry was then conducted using a Ventana BenchMark GX instrument (Roche, Basel, Switzerland) with an anti-FAM111B or anti-Ki-67 antibody. Regions where the FAM111B LI was >10% and where it was <10% were defined as areas of high or low LI, respectively, as the median FAM111B LI in all LUAD cases was 10%. Regions where the Ki-67 LI was >10% and where it was <10% were defined as areas of high or low LI, respectively, as the median Ki-67 LI in all LUAD cases was 10%. Regarding the classification of the LUAD subtype, the proportion of cells that exceeded 50% of a clinical specimen was regarded as the subtype of the tumor for a particular patient.

2.7 | Immunocytochemistry

Cells were rinsed in PBS, fixed in 4% formaldehyde in PBS for 10 min, and permeabilized with 0.05% Triton X-100 in PBS for 1 min. Immunocytochemistry using an anti-FAM111B antibody was conducted with the EnVision + Kit (Dako), in accordance with the manufacturer's instructions.

2.8 | Preparation of total cell extracts

Cells were rinsed 3 times with PBS and lysed in ice-cold lysis buffer (1% NP-40, 10 mmol/L Tris-HCl, 200 mmol/L NaCl, 1 mmol/L ethylenediaminetetraacetic acid) containing ethylenediaminetetraacetic acid-free complete protease inhibitor cocktail (Roche) for 20 min. The soluble fractions of cell lysates were isolated by centrifugation at 15 000 g for 10 min in a microcentrifuge.

2.9 | Isolation of nuclear and cytoplasmic fractions

Cells were rinsed 3 times with ice-cold PBS. Nuclear and cytosolic fractions were prepared using an NE-PER Nuclear Cytoplasmic Extraction Reagent Kit (Pierce, Rockford, IL, USA), in accordance with the manufacturer's instructions.

2.10 | Immunoprecipitation

A549 cells were transfected with FAM111B-FLAG and/or p16-V5 expression plasmid constructs. Cells were lysed in buffer comprising 1% NP-40, 10 mmol/L Tris-HCl, 150 mmol/L NaCl, 0.5 mmol/L phenylmethylsulfonyl fluoride, 5 µg/mL aprotinin, 5 µg/mL leupeptin, and protease inhibitor cocktail (Roche). Cell lysates were incubated with protein G-Sepharose beads (GE Healthcare Life Sciences, Chicago, IL, USA) plus an anti-FLAG and/or anti-V5 antibody for 3 h at 4°C. After beads had been washed 5 times with lysis buffer, immunoprecipitates were isolated by sodium dodecyl sulfate-polyacrylamide gel electrophoresis (SDS-PAGE) and immunoblotted with an anti-FLAG or anti-V5 antibody.

2.11 | Western blotting

Proteins were analyzed by sodium dodecyl sulfate-polyacrylamide gel electrophoresis and immunoblotting, in accordance with a standard protocol.[14] Band intensities were quantified by densitometry using ImageJ software (https://imagej.nih.gov/ij/).

2.12 | RNA sequencing of FFPE samples

We prepared 20 10-µm-thick FFPE sections from each of 2 LUAD tumors that included lepidic- or papillary-predominant adenocarcinoma components. Approximately 10 × 10-mm tumor areas that included lepidic- or papillary-predominant adenocarcinoma components were estimated visually and dissected using a blade, then collected and subjected to RNA-seq analysis. Total RNA was extracted from the cells using the miRNeasy FFPE Kit (Qiagen, Hilden, Germany), in accordance with the manufacturer's protocol. Next-generation sequencing (NGS) library preparation was performed using the TruSeq RNA Access Library Prep Kit (Illumina, San Diego, CA, USA), in accordance with the manufacturer's instructions. Sequencing was performed on
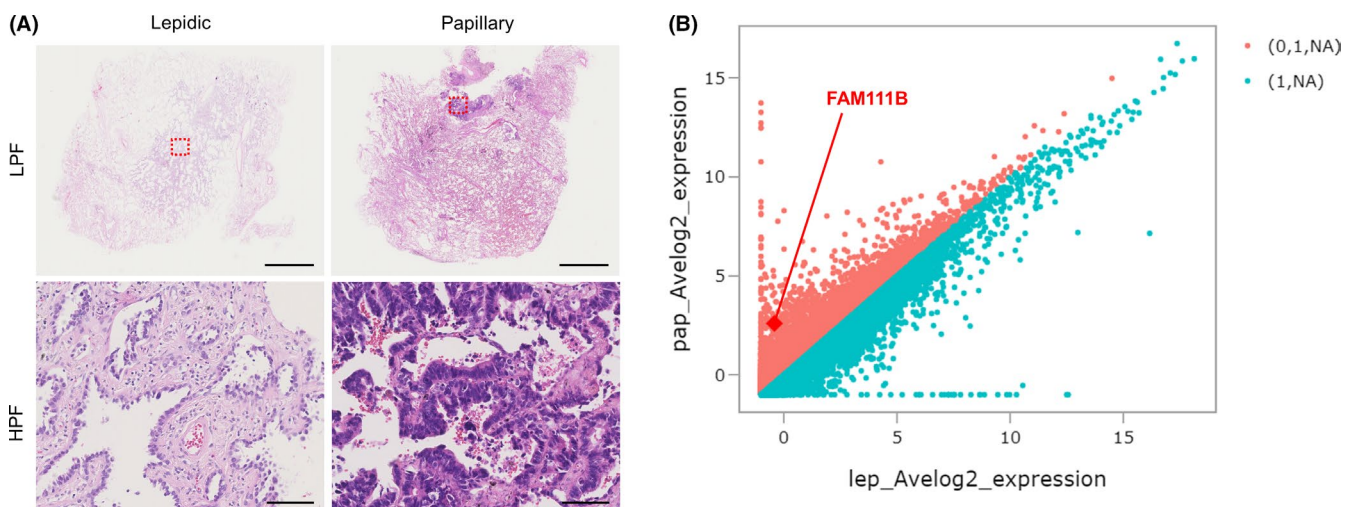
FIGURE 1 RNA-seq screening of human lung adenocarcinoma (LUAD) tissues. A, Hematoxylin and eosin sections of lepidic- and papillary-predominant LUAD used for RNA-seq analysis. The areas of tumor lesions were dissected and subjected to RNA-seq. Family with sequence similarity 111 member B (FAM111B) is indicated by the red spot. B, RNA-seq results plotted as a scatterplot matrix. FAM111B expression was higher in papillary-predominant LUAD than in lepidic-predominant LUAD. LPF, low-power field. HPF, high-power field. Scale bars, 5 mm (LPF) and 100 µm (HPF)

an Illumina HiSeq 2500 platform in 75-base single-end mode with Illumina Casava 1.8.2 software for base calling. Sequenced reads were mapped to the human reference genome sequence (hg19) using TopHat v.2.0.13 software, in combination with Bowtie 2 v.2.2.3 and SAMtools v.0.1.19. Fragments per kilobase of exon per million mapped fragments were calculated using Cufflinks v.2.2.1. Raw data were deposited in the NCBI Gene Expression Omnibus database (GSE143501).

2.13 | Generation of FAM111B-KO A549 cell lines

FAM111B in A549 cells was disrupted using the TrueGuide™ CRISPR/Cas9 system (Invitrogen, Carlsbad, CA, USA), in accordance with the manufacturer's instructions. The control crRNA (Invitrogen TrueGuide™ Synthetic crRNA, Negative Control, Human and Mouse) was annealed with tracrRNA. A549 cells were co-transfected with the crRNA:tracrRNA complex as the negative control (NC). A549 parent cells (PC) were used as another NC.

2.14 | siRNA-mediated silencing of FAM111B in LUAD cell lines

HCC827, H1650, and H1792 cells seeded at 70% confluence were transfected with an FAM111B-targeting siRNA (Silencer Select s51538, s51539; Thermo Fisher Scientific, Waltham, MA, USA) or non-targeting control siRNA (AM4611; Thermo Fisher Scientific), using Lipofectamine RNAiMAX reagent (Thermo Fisher Scientific) at a final concentration of 50 nmol/L. Sequences of the FAM111B-targeting siRNAs were 5′-GCAATTCAACATATATAAAA-3′ (s51538) and 5′-CAGCTTACATATTATAGCAA-3′ (s51539). HCC827, H1650, and H1792 PC were used as the NCs.

2.15 | Cell proliferation assay

Cells were counted using a Muse™ Cell Analyzer (Merck Millipore, Burlington, MA, USA). Cell proliferation was assayed using the Premix WST-1 Cell Proliferation Assay System (TaKaRa, Shiga, Japan), in accordance with the manufacturer's protocol.

2.16 | Cell migration assay

Cell migration was evaluated by scratch wound-healing assay, in accordance with the standard protocol.[14] Distances between cells were measured using ImageJ software.

2.17 | Cell invasion assay

Invasion capability was evaluated by in vitro cell invasion assay using Corning BioCoat Matrigel Invasion Chambers with an 8.0-μm

polyethylene terephthalate membrane (Corning, Corning, NY, USA), in accordance with the standard protocol.[14] The numbers of invading cells were calculated by averaging 4 random counts per 10 high-power fields at ×200 magnification per membrane and calculating the average of 3 membranes.

2.18 | Cell cycle analysis

Cell cycle analysis was conducted using a Muse Cell Cycle Kit and a Muse Cell Analyzer (Merck Millipore), in accordance with the manufacturer's instructions.

TABLE 1 Statistics for family with sequence similarity 111 member B (FAM111B) LI and clinicopathological features

Factors	No. of cases	FAM111B LI (%)	*P*-value
Age			
<70	39	16.5	.69
≥70	56	16.1	
Sex			
Female	32	11.9	.011
Male	63	19.8	
Tumor size			
<30 mm	53	13.5	.0053
≥30 mm	42	21.8	
T classification			
pT1	55	14.3	.023*
pT2	29	22.4	
pT3	6	21.7	
pT4	5	13.0	
Lymphovascular invasion			
No	71	14.3	<.001
Yes	24	25.8	
N classification			
pN0	84	16.0	.033**
pN1	11	25.9	
pN2	0	0	
pN3	0	0	
Recurrence			
No	83	16.6	.40
Yes	12	21.3	
Pathological staging			
Stage I	68	14.5	.006***
Stage II	16	25.6	
Stage III	11	21.3	
Stage IV	0	0	

*P < .05 when compared between pT1 and pT2-pT4.

**P < .05 when compared between pN0 and pN1-pN3.

***P < .01 when compared between Stage I and Stages II-IV.

2.19 | Statistical analysis

The database was created using Microsoft Excel (Microsoft Corp., Redmond, WA, USA) and analyzed using JMP Pro 13 (SAS Institute, Cary, NC, USA). When 2 groups were normally distributed with or without equal variances, Student t test was applied. Co-occurrence of the Ki-67 LI with the FAM111B LI was assessed using the two-sided χ^2 test.

3 | RESULTS

3.1 | FAM111B expression is correlated with malignant progression of LUAD

First, we performed RNA-seq using human FFPE tissue specimens to compare gene expression profiles between lepidic-predominant adenocarcinomas and papillary-predominant adenocarcinomas
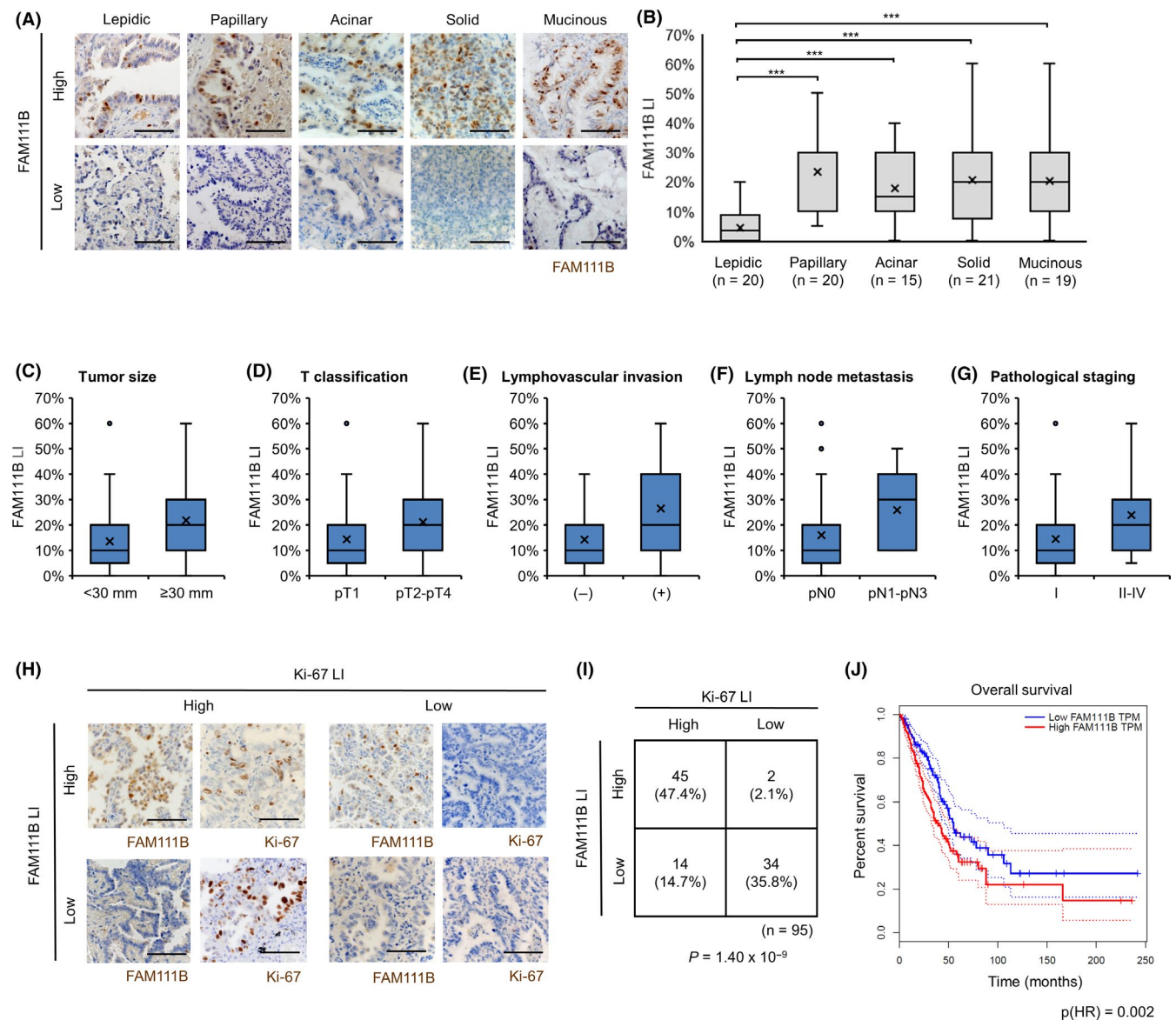
FIGURE 2 Immunohistochemical analysis of FAM111B in clinical lung adenocarcinoma (LUAD) specimens. A, Representative immunohistochemically stained images of family with sequence similarity 111 member B (FAM111B) in lepidic-, papillary-, acinar-, solid-, and mucinous-predominant adenocarcinomas. B, Statistical analysis based on the FAM111B labeling index (LI). C-G, Correlations between FAM111B expression and tumor size (C), T classification (D), presence/absence of lymphovascular invasion (E), N classification (F), and pathological staging (G) according to FAM111B LI. H, Representative immunohistochemically stained images of tumors with a high or low LI of FAM111B or Ki-67. I, Correlation between FAM111B LI and Ki-67 LI. J, Kaplan-Meier plots for FAM111B expression in LUAD derived from Gene Expression Profiling Interactive Analysis (http://gepia.cancer-pku.cn). The dotted line was estimated by the 95% confidence interval. Significance was calculated by two-sided χ^2 test. Scale bar, 100 μm (A, G). Student t test: $*P < .05$, $**P < .01$, $***P < .001$

(A)

(B)

FAM111B

(C)

(D)

(E)
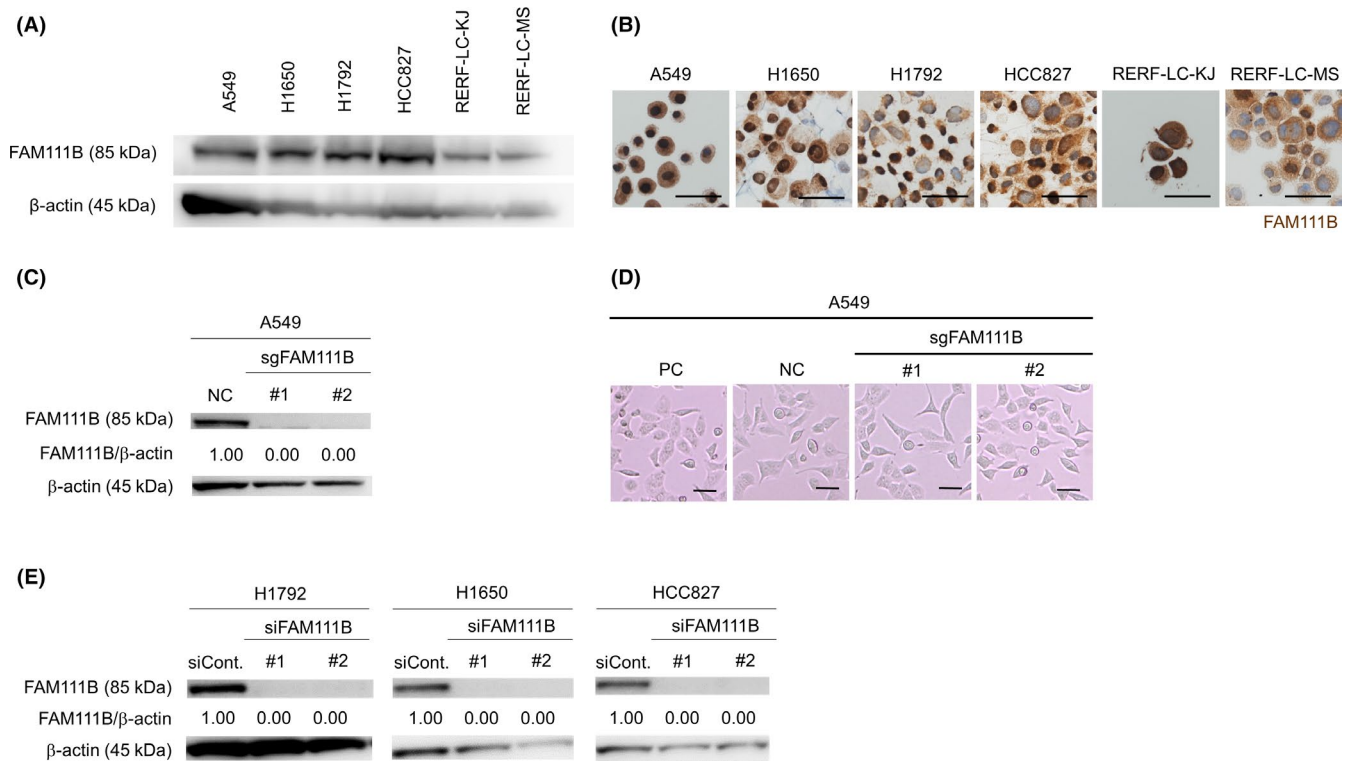
FIGURE 3 Generation of family with sequence similarity 111 member B (FAM111B)-knockout LUAD cells. A, Immunoblotting of FAM111B in lung adenocarcinoma (LUAD) cells. B, Representative immunocytochemical images of FAM111B in LUAD cells. C, Immunoblotting of FAM111B in knockout A549 cells generated using the CRISPR/Cas9 system. The relative quotient of 2 knockout cell clones (sgFAM111B#1 and #2) is presented as the ratio to the relative quotient of NC cells. NC; Negative control. D, Morphological images of A549 cells. PC; A549 parent cells, NC; Negative control. E, Representative immunoblots of LUAD cells transfected with 2 siRNA duplexes specific for FAM111B (siFAM111B #1 and #2) or a non-targeting control siRNA (siCont). Scale bars, 100 μm (B) and 200 μm (D)

(Figure 1). Among the expressed genes, we focused on *FAM111B* due to its histopathological significance. We examined FAM111B expression in 95 LUAD clinical specimens by immunohistochemistry. The clinicopathological features of these tumors are shown in Table 1. Interestingly, FAM111B staining was among the specimens. Some cancer cells in the specimen were positive for FAM111B and the protein was localized mainly in the nucleus (Figure 2A). In addition, FAM111B LI was significantly higher in papillary-predominant adenocarcinomas than in lepidic-predominant adenocarcinomas (Figure 2B), consistent with the RNA-seq results. Moreover, the FAM111B LI was higher in acinar-, solid-, and mucinous-predominant adenocarcinomas than in lepidic-predominant adenocarcinomas (Figure 2B). FAM111B expression was associated with tumor size, T classification, frequency of lymphovascular invasion, N classification, and pathological staging (Figure 2C-G) We also investigated the correlation between the expression pattern of FAM111B and the expression pattern of a proliferation marker, Ki-67. Immunohistochemistry revealed a significant correlation between the FAM111B LI and the Ki-67 LI (Figure 2H,I). Additionally, gene expression analysis using publicly available data sets pipelined through Gene Expression Profiling Interactive Analysis showed that expression of FAM111B influenced the overall survival of patients with LUAD (p(HR) = 0.002) (Figure 2J). Therefore, FAM111B expression was higher in papillary-, acinar-, solid-, and mucinous-predominant adenocarcinomas than in lepidic-predominant

adenocarcinomas and was significantly correlated with malignant progression of LUAD.

3.2 | FAM111B is associated with proliferation of *KRAS*-driven LUAD under serum-starvation conditions

To investigate the molecular function of FAM111B in LUAD, we established a FAM111B-knockout (FAM111B-KO) LUAD cell line using the CRISPR/Cas9 system. Immunoblotting and immunocytochemistry showed that several LUAD cell lines exhibited sufficient FAM111B expression (Figure 3A,B). We disrupted *FAM111B* in A549 cells, a commonly used LUAD cell line, to generate FAM111B-KO cells (Figures 3C and S1). There were no significant differences in shape among 2 independent clones of FAM111B-KO cells (sgFAM111B#1 and #2), FAM111B wild-type PC, and a negative control sgRNA-transfected clone (NC) (Figure 3D). In addition, knockdown by siRNA attenuated FAM111B expression levels in H1792, H1650, and HCC827 cells (Figure 3E).

Next, we investigated the functional importance of FAM111B in LUAD using the above knockout or knockdown cell lines. No significant differences in proliferation were observed among FAM111B-KO, PC, and NC A549 cells cultured in standard DMEM supplemented with 10% FCS. However, FAM111B-KO A549 cells
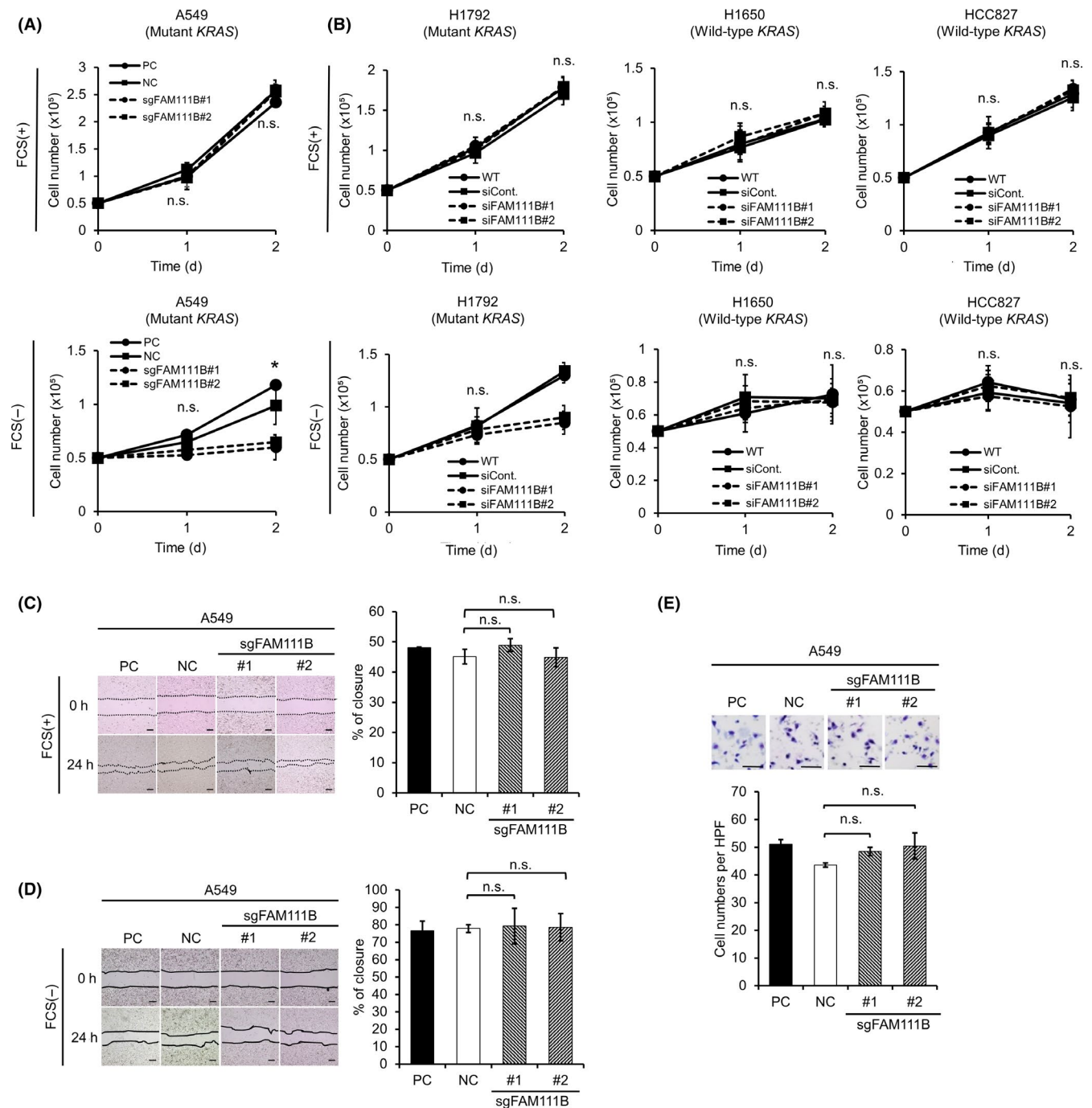
FIGURE 4 Family with sequence similarity 111 member B (FAM111B)-knockout and FAM111B-knockdown lung adenocarcinoma (LUAD) cells showed reduced proliferation under FCS-starvation conditions. A, Cell proliferation. Cells (5×10^4) were seeded for 6 h, the medium was replaced by DMEM with or without FCS, and cells were enumerated. B, Proliferation of FAM111B-knockdown LUAD cells. C, D, Cell motility by wound-healing assay. A549 cell layers were wounded using a pipette tip. The migration distance was calculated by subtracting the width of the wound at 24 h from the width at 0 h. The migration distance of the control siRNA was expressed as 100%. Dashed line indicates the cell front. PC, A549 parent cells; NC, Negative control. E, Invasion evaluated by Transwell Matrigel invasion assay. Representative images of invading A549 cells are shown. Invasive cells were counted in 10 random high-power fields per well. Data are means ± SDs from 3 independent experiments. Scale bar, 200 μm (C-E). PC, A549 parent cells; NC, Negative control. Student t test: *$P < .05$. n.s., not significant

showed attenuated proliferation when cultured in DMEM without FCS (Figure 4A). To confirm this, we evaluated the proliferation of FAM111B-knockdown H1792, H1650, and HCC827 cells. Interestingly, FAM111B-knockdown H1792 cells, which harbor a

$KRAS$ mutation, displayed attenuated proliferation when cultured in DMEM without FCS, while FAM111B-knockdown H1650 and HCC827 cells with wild-type $KRAS$ did not, even under FCS-free conditions (Figure 4B). Because A549 cells have a mutant $KRAS$,

FIGURE 5 The relation between family with sequence similarity 111 member B (FAM111B) and p16. A, Proportions of cells in S, G2/M, or G0/G1 phases. B, Cell cycle phase distribution of PC, NC, KO (sgFAM111B#1 and #2) A549 cells. A, B, Cells (5×10^5) were seeded for 6 h, the medium was replaced by DMEM with or without FCS, and a cell cycle analysis was performed after 48 h. C, D, Expression levels of the indicated factors associated with the cyclin D1-CDK4-dependent cell cycle were evaluated by immunoblotting of nuclear and cytoplasmic extracts of A549 cells. Data are means ± SDs from 3 independent experiments. *$P < .05$, Student t test. A-D, PC, A549 parent cells; NC, Negative control. E, F, Representative immunohistochemical images of FAM111B and p16 in human LUAD tissue. Regions where the FAM111B LI was >10% and where it was <10% were defined as areas of high and low LI, respectively. Correlation between p16 LI and FAM111B LI in LUAD tissues of 95 tumors. Student t test. Scale bars, 500 μm (LPF) or 50 μm (HPF)

FAM111B is likely to contribute to *KRAS*-driven LUAD. The phenotype of FAM111B-KO A549 cells was reproducible in WST-1 cell proliferation assays (Figure S2). In contrast, the proliferation of FAM111B-KO A549 cells was not attenuated under glucose starvation or hypoxic conditions (Figure S3). Furthermore, in vitro scratch wound-healing and invasion assays demonstrated that depletion of FAM111B in A549 cells did not affect motility or invasion (Figure 4C-E). Therefore, FAM111B is associated with proliferation/survival in the presence of serum starvation, specifically in *KRAS*-driven LUAD.

3.3 | FAM111B is involved in p16 degradation and positively regulates the cyclin D1-CDK4-dependent cell cycle

We next examined the effect of FAM111B depletion on cell cycle progression in A549 cells. The proportions of S-phase and G2/M-phase cells were significantly reduced in FAM111B-KO A549 cells, compared with PC and NC cells in FCS-free medium, whereas no such difference was observed in DMEM with FCS (Figure 5A,B). In contrast, the proportion of G0/G1-phase cells was elevated in FAM111B-KO A549 cells cultured in FCS-free medium (Figure 5A,B). Therefore, the reduced proliferation of FAM111B-KO A549 cells was due to G0/G1 cell cycle arrest.

When mutant *KRAS*-dependent transcription and translational activation occurs upstream of cyclin D1, the cyclin D1-CDK4/6 complex is formed, which phosphorylates Rb1.[15] Phosphorylated Rb1 dissociates from E2F; the resultant free form of E2F activates its target genes, enabling the G1/S-phase transition.[15] p16 (CDKN2A) inhibits CDK4 and CDK6, and its germline mutations are associated with various tumors including malignant melanoma, pancreatic cancer, and glioblastoma. Therefore, we hypothesized that FAM111B is involved in this pathway.

Immunoblotting revealed that FAM111-KO A549 cells exhibited higher p16 expression than NC cells in DMEM (Figure 5C,D). Additionally, quantitative analysis of immunoblot band intensities demonstrated that the phosphorylation level of Rb was significantly reduced in FAM111-KO A549 cells, compared to NC cells, under FCS-starvation conditions. E2F-1 expression was also attenuated in FAM111B-KO cells (Figure 5C,D). The levels of p53, p15, Cyclin D1, and CDK4 did not differ significantly between FAM111-KO and NC cells (Figure 5C,D). Notably, no marked differences were observed in the Akt, mTOR, and Erk1/2 phosphorylation levels between FAM111B-KO and NC cells (Figure S4). Therefore, FAM111B-KO

cells exhibited reduced expression of p16 and impaired inhibition of the cyclin D1-CDK4 complex, which led to attenuation of both Rb phosphorylation and E2F-1 activation, resulting in prolonged G0/G1 arrest.

We next examined the relationship between FAM111B and p16 expression in human LUAD tissues by immunohistochemistry. Consistent with the immunoblotting data, tumor regions with a high FAM111B LI coincided with those with a low p16 LI (Figure 5E,F).

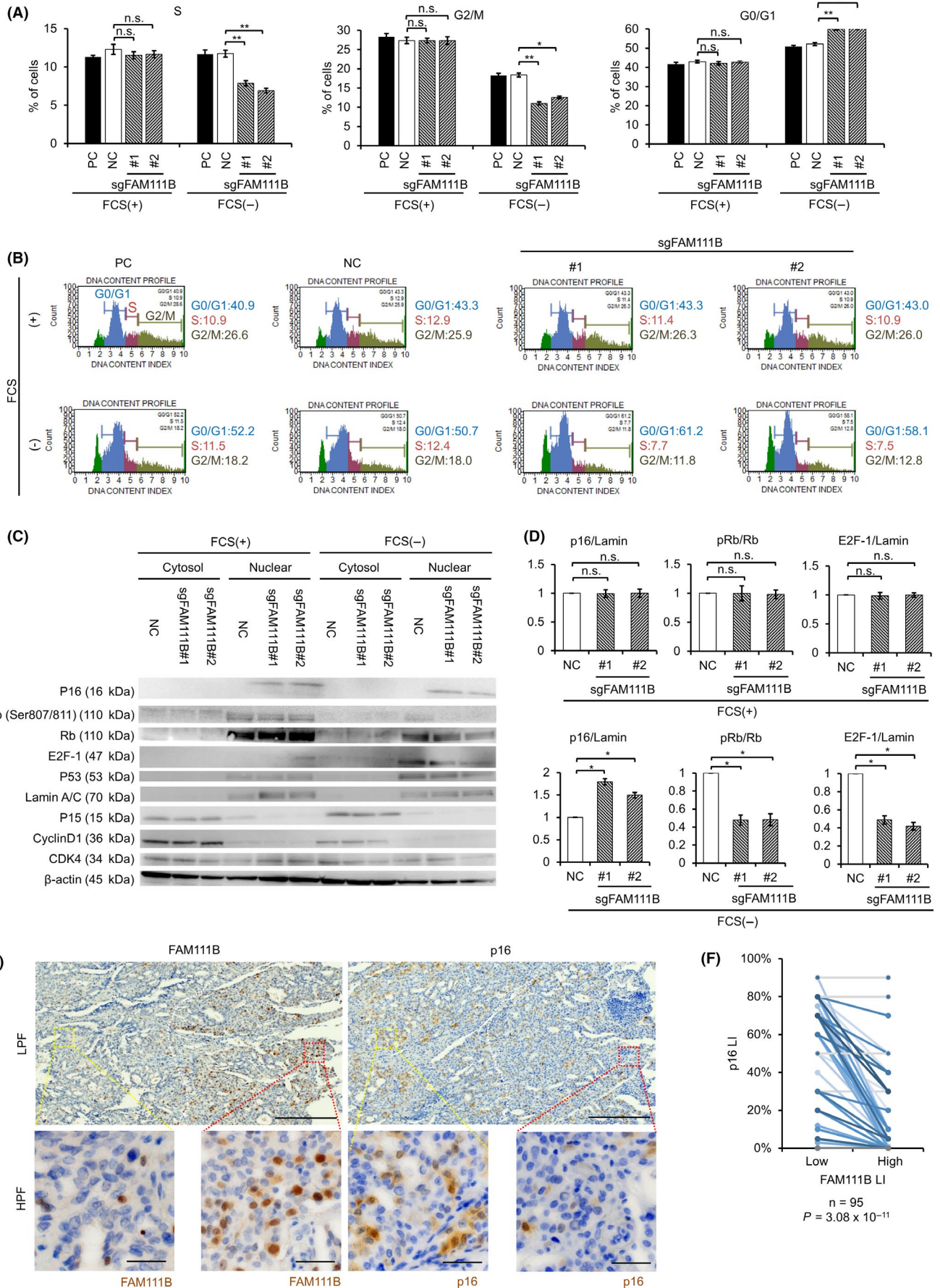## 3.4 | The trypsin protease domain is essential for the function of FAM111B

FAM111B contains a putative trypsin-like cysteine/serine peptidase domain (TPD) in the C-terminus,[5] suggesting degradative activity. Therefore, we hypothesized that FAM111B modulates the level of p16 by mediating degradation of p16. To evaluate this hypothesis, we co-transfected plasmid constructs expressing FLAG-tagged FAM111B and/or V5-tagged p16 into A549 cells and performed co-immunoprecipitation; FAM111B directly bound to p16 (Figure 6A). To confirm the functional importance of the TPD in FAM111B, we generated a plasmid construct encoding FAM111BΔTPD (a mutant FAM111B lacking the peptidase domain), as well as a construct encoding full-length FAM111B (Figure 6B). As expected, the reduced proliferation of FAM111B-KO cells could not be rescued by expression of FAM111BΔTPD, whereas expression of full-length FAM111B successfully rescued their phenotype (Figure 6C). Additionally, in A549 cells transfected with a plasmid harboring full-length FAM111B, the p16 protein level was reduced to a level similar to that of NC cells under serum-starvation conditions (Figure 6D). These results supported the hypothesis that FAM111B degrades p16.

4 | DISCUSSION

We examined the relationship between FAM111B expression in human LUAD tissues and clinicopathological parameters in affected patients. FAM111B expression was correlated with malignant progression. Additionally, FAM111B modulated the p16 level by mediating its degradation, thereby altering the growth and cell cycle progression of *KRAS*-driven LUAD cells.

We evaluated the clinicopathological importance of FAM111B in human LUAD specimens by immunohistochemistry.
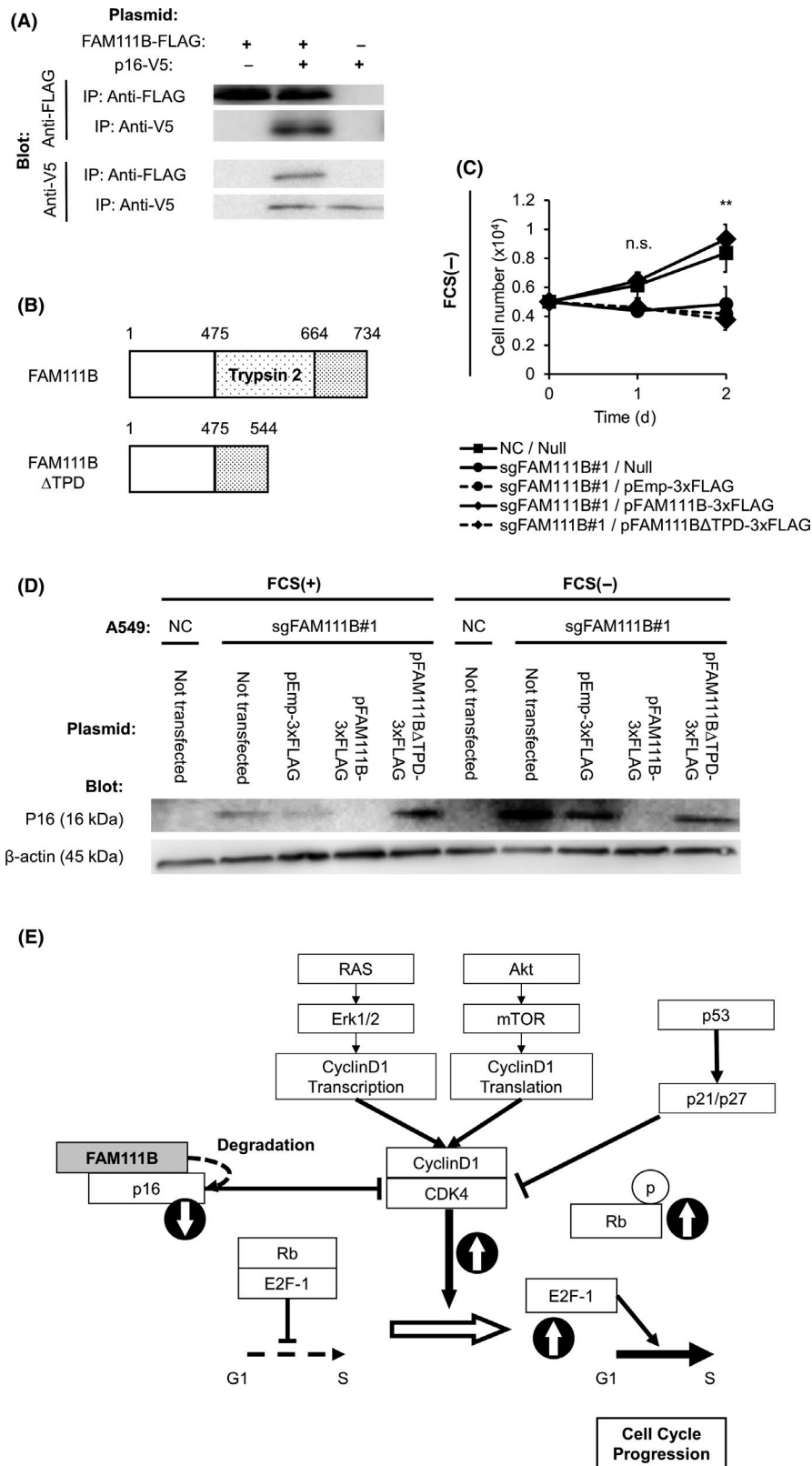
FIGURE 6 The trypsin protease domain is essential for the activity of family with sequence similarity 111 member B (FAM111B). A, Interaction between FAM111B and p16. Plasmid constructs expressing FLAG-tagged FAM111B and/or V5-tagged p16 were co-transfected into A549 cells, which were then subjected to immunoprecipitation and immunoblotting using the indicated antibodies. B, Schematic of human FAM111B (NP_945185.1) protein and its mutant lacking the trypsin-like protease domain, FAM111BΔTPD. C, A549 cells were transfected with the indicated plasmids. After 24 h, the medium was replaced by DMEM with or without FCS, and cells were enumerated. PC, A549 parent cells; NC, Negative control. D, Immunoblotting of p16. Cells were transfected with the indicated plasmids for 24 h and collected; then, 5×10^4 cells were seeded for 6 h. The medium was replaced by DMEM with or without FCS and cells were enumerated. PC, A549 parent cells; NC, Negative control. E, Schematic of the role of FAM111B in LUAD cells. Data are representative of 3 independent experiments. **$P < .01$, Student t test

Papillary-predominant solid-predominant, acinar-predominant, and invasive mucinous adenocarcinomas exhibited significantly higher FAM111B expression, compared with lepidic-predominant adenocarcinomas. Sun et al reported a correlation between FAM111B expression in LUAD tissues and histological differentiation of these tissues, using a three-tiered grading system (well, moderately, or poorly differentiated adenocarcinoma).[13] However, FAM111B expression in the subtypes of LUAD was not evaluated. In the present study, FAM111B expression was correlated with tumor size, T classification, frequency of

lymphovascular invasion, and N classification. Sun et al reported similar results.[13]

We also generated FAM111B-KO A549 cells using the CRISPR/Cas9 system. In vitro experiments using these cell lines demonstrated that FAM111B contributes to the proliferation of LUAD cells. Interestingly, attenuated proliferation of FAM111B-KO cells was observed only under serum-starvation conditions. Sun et al reported attenuated proliferation, even under standard culture conditions.[13] The discrepancy might be due to the use of different methods for reduction of FAM111B expression; transient RNA silencing by siRNA vs generation of stable FAM111B-deficient A549 cells using the CRISPR/Cas9 system. Knockdown by siRNA reduces gene expression only at the mRNA level, while knockout using the CRISPR/Cas9 system completely and permanently silences the gene at the DNA level.[16] Therefore, our results are presumably more robust. Phenotypes reproducible in specific situations, such as proliferation/survival under nutrient-starvation conditions, cannot be evaluated unless a gene is permanently silenced. Notably, siRNA has greater off-target effects, which may result in a modified phenotype.

Interestingly, in vitro functional assays using FAM111B-knockdown H1792, H1650, or HCC827 cells demonstrated that FAM111B is important only in *KRAS*-driven LUAD. Indeed, in human LUAD tissues, FAM111B expression was significantly higher in invasive mucinous carcinomas (a subtype of *KRAS*-driven LUAD) than in lepidic-predominant adenocarcinomas.

Furthermore, we revealed that FAM111B regulates cell cycle progression in LUAD by modulating the p16 level through degradation of p16. Sun et al reported that FAM111B functions downstream of p53 and is involved in growth, G2-M arrest, and apoptosis[13]; however, they did not evaluate the underlying molecular mechanism. Here, we demonstrated that G0/G1 arrest occurred in FAM111B-KO cells due to elevated p16 expression and the resulting reductions of Rb phosphorylation and E2F-1 activation. In addition, FAM111B bound directly to and degraded p16. The enzymatic specificity of FAM111B is defined by its binding specificity for p16. Moreover, full-length FAM111B, but not FAM111BΔTPD, rescued the phenotype of FAM111B-KO cells, supporting the hypothesis that protease activity of FAM111B is important for LUAD. Sun et al [13] reported that p53 acts directly on FAM111B to suppress the cell cycle; however, definitive evidence of this is lacking. Further research is needed to confirm whether FAM111B is directly involved in the p53-dependent cell cycle and apoptosis. To the best of our knowledge, this is the first report of the novel function of FAM111B in regulation of cell cycle progression.

In summary, FAM111B expression was higher in papillary-predominant adenocarcinomas than in lepidic-predominant adenocarcinomas. Furthermore, in *KRAS*-driven LUAD cells, FAM111B degraded p16 and positively regulated cell cycle progression and proliferation by enhancement of cyclin D1-CDK4 activity. This is the first report of the function of FAM111B in cancer biology.

CONFLICT OF INTEREST

The authors have no conflict of interest.

AUTHORS CONTRIBUTION

Keisuke Kawasaki: Experiments, data curation, project administration, writing—original draft, and writing—review and editing. Satoshi Nojima: Data curation, methodology, project administration and writing—review and editing. Daisuke Okuzaki: DNA microarray screening and data analyzing. Sachiko Hijiki: Experiments and data curation. Shinichiro Tahara, Kenji Ohshima, Takahiro Matsui, Yumiko Hori, Masako Kurashige, Daisuke Umeda, Hiroki Kiyokawa and Kansuke Kido: Providing advice on project planning and data interpretation. Eiichi Morii: Conceptualization, supervision, project administration, funding acquisition and writing—review and editing.

ORCID

Keisuke Kawasaki https://orcid.org/0000-0001-7647-7890
Shinichiro Tahara https://orcid.org/0000-0001-6134-3275

REFERENCES

1. Jemal A, Siegel R, Ward E, et al. Cancer statistics, 2008. *CA Cancer J Clin*. 2008;58:71-96.
2. Druker BJ, Talpaz M, Resta DJ, et al. Efficacy and safety of a specific inhibitor of the BCR-ABL tyrosine kinase in chronic myeloid leukemia. *N Engl J Med*. 2001;344:1031-1037.
3. Kuhn E, Morbini P, Cancellieri A, Damiani S, Cavazza A, Comin CE. Adenocarcinoma classification: patterns and prognosis. *Pathologica*. 2018;110(1):5-11.
4. Silver SA, Askin FB. True papillary carcinoma of the lung: a distinct clinicopathologic entity. *Am J Surg Pathol*. 1997;21:43-51.
5. Sica G, Yoshizawa A, Sima CS, et al. A grading system of lung adenocarcinomas based on histologic pattern is predictive of disease recurrence in stage I tumors. *Am J Surg Pathol*. 2010;34:1155-1162.
6. Song Z, Zhu H, Guo Z, Wu W, Sun W, Zhang Y. Prognostic value of the IASLC/ATS/ERS classification in stage I lung adenocarcinoma patients – based on a hospital study in China. *Eur J Surg Oncol*. 2013;39:1262-1268.
7. Warth A, Muley T, Meister M, et al. The novel histologic International Association for the Study of Lung Cancer/American Thoracic Society/European Respiratory Society classification system of lung adenocarcinoma is a stage-independent predictor of survival. *J Clin Oncol*. 2012;30:1438-1446.
8. Hu HD, Wan MY, Xu CH, et al. Histological subtypes of solitary pulmonary nodules of adenocarcinoma and their clinical relevance. *J Thorac Dis*. 2013;5:841-846.
9. Travis WD, Travis LB, Devesa SS. Lung cancer. *Cancer*. 1995;75:191-202.
10. Rodenhuis S, Van De Wetering ML, Mooi WJ, Evers SG, van Zandwijk N, Bos JL. Mutational activation of the K-ras oncogene. A possible pathogenetic factor in adenocarcinoma of the lung. *N Engl J Med*. 1987;317:929-935.

11. Mercier S, Küry S, Shaboodien G, et al. Mutations in FAM111B cause hereditary fibrosing poikiloderma with tendon contracture, myopathy, and pulmonary fibrosis. *Am J Hum Genet*. 2013;93(6):1100-1107.

12. Küry S, Mercier S, Shaboodien G, et al. CUGC for hereditary fibrosing poikiloderma with tendon contractures, myopathy, and pulmonary fibrosis (POIKTMP). *Eur J Hum Genet*. 2015;24(5):779.

13. Sun H, Liu K, Huang J, et al. FAM111B, a direct target of p53, promotes the malignant process of LUAD. *Onco Targets Ther*. 2019;12:2829-2842.

14. Ohshima K, Nojima S, Tahara S, et al. Argininosuccinate Synthase 1-Deficiency Enhances the Cell Sensitivity to Arginine through Decreased DEPTOR Expression in Endometrial Cancer. *Sci Rep*. 2017;30(7):45504.

15. Maria S, Gregory AD, David EP, et al. Cyclin alterations in diverse cancers: outcome and co-amplification network. *Oncotarget*. 2015;6(5):3033-3042.

16. Wang T, Wei JJ, Sabatini DM, Lander ES. Genetic screens in human cells using the CRISPR-Cas9 system. *Science*. 2014;343(6166):80-84.

SUPPORTING INFORMATION

Additional supporting information may be found online in the Supporting Information section.